UNCECOMP 2015
1st ECCOMAS Thematic Conference on
Uncertainty Quantification in Computational Sciences and Engineering
M. Papadrakakis, V. Papadopoulos, G. Stefanou (eds.)
Crete Island, Greece, 25–27 May 2015

OPTIMAL SENSOR PLACEMENT FOR THE MODAL IDENTIFICATION OF AN INNOVATIVE TIMBER STRUCTURE

C. Leyder[1], V. Ntertimanis[1], E. Chatzi[1] and A. Frangi[1]

[1]ETHZ Institute of Structural Engineering
Stefano-Franscini Platz 5
8093 Zürich
Switzerland
e-mail: {leyder,ntertimanis,chatzi,frangi}@ibk.baug.ethz.ch

Keywords: Optimization, Sensor-position, Innovative Timber Structure, Modal testing

Abstract. *This paper aims at determining an optimal grid of acceleration sensors for the accurate estimation of modal data from an innovative timber-hybrid structure. As the knowledge on the full-scale behaviour of such structures is limited thus far, an extensive identification campaign on an innovative timber building, the ETH House of Natural Resources, is currently being carried out at ETH Zürich. In conjunction with this campaign an optimal placement for modal identification sensors is undertaken, in order to extract the maximum possible information from a minimal number of sensors. The entire structure is modelled in SAP2000 and the modal information (frequencies and mode shapes) is extracted from the software. The obtained mode shapes are then utilized as the input to the sensor placement problem. Three widely accepted sensor placement methods are implemented and assessed, namely, the effective independence method (EFI), the driving point residue EFI method (EFI-DPR) and the maximum kinetic energy method (MKE). The optimization algorithms identify the most relevant degrees of freedom, which should be monitored during the testing campaign.*

1 INTRODUCTION

One main focus in timber engineering is the development of innovative structures, which are efficient and reliable throughout their life–cycle. To this end, the implementation of hardwood elements opens up a whole range of new possibilities for timber structures. New structural systems are mostly developed and tested under laboratory conditions, i.e., in small to mid-scale and in a controlled environment. The knowledge concerning the structural behaviour in an actual–scale building situation as well as the long-term use is limited. Therefore a pilot building demonstrating the implementation of hardwood for structural elements has been realized at ETH Zürich, under a project titled "ETH House of Natural Resources (ETH HoNR)" [1]. The building allows for the quantification of the structural behaviour of several innovative structures in a real building situation.

In order to gain further information about the novel structural systems that have been adopted in the ETH HoNR building, an extensive modal testing campaign was conducted on the structure, resulting in the modal assessment of the innovative hardwood structure. When carrying out modal vibration tests on little so far explored structures, the optimal placement of sensors is a main subject. Indeed the issue of optimal sensor placement (OSP) is not a trivial one as it relies on the extraction of salient features that determine structural behaviour and that are not straightforwardly known a-priori. Therefore sensor placement optimization algorithms can be implemented either on modal data determined by tests (if available), or based on an a-priori finite element model. For the ETH HoNR structure several models based on analytical relations and small-scale tests have been developed and herein used for the determination of optimal sensor positions. As described in the review paper by [2], a multitude of sensor placement optimization algorithms are already available in the literature. Here the focus is put on the effective independence method (EFI), the driving point residue EFI method (EFI-DPR), the maximum kinetic energy method (MKE), which are deemed as most suitable. A short review of optimal sensor placement techniques and their implementation for a bridge structure is documented in [3]. Glassburn and Smith [4] additionally document several optimal sensor placement methods for implementation on a truss structure.

The paper is organized as follows: Sec. 2 describes the innovative timber structure and the corresponding numerical model for which the OSP methodologies are applied. A brief introduction of the adopted OSP methods and the results of their application to the structure considered herein is taking place in Sec. 3. Section 4 discusses on the OSP campaign results and, finally, Sec. 5 provides some concluding remarks along with further research efforts undertaken by the group.

2 INNOVATIVE TIMBER STRUCTURE

2.1 Post-tensioned timber frame

The main structural unit of the ETH HoNR is a post-tensioned timber frame. This has been developed and tested in full scale in the IBK Structures laboratory of ETH Zürich [5]. In New-Zealand a similar system, known as Pres-lam was invented and implemented in several buildings [6, 7]. Advantages of the post-tensioned frame comprise its high ductility, which allows for a self-centring moment-rotation behaviour. In order to analyse the behaviour of the post-tensioned timber frame, first a single beam-column specimen was tested in the laboratory of ETH Zrich. Relying on these tests a model for the behaviour of this special-type joint could be developed. In a second step, an entire three-bay frame was tested with a pushover test, in order to verify the applicability of the derived single joint behaviour within the context of an

Figure 1: 2D Frame a) laboratory setup b) Model in SAP2000

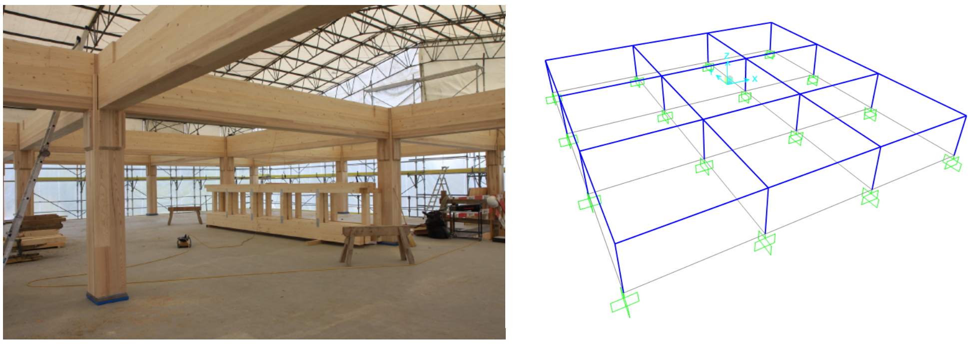

Figure 2: 3D Frame a) Construction Site b) Model in SAP2000

entire frame [8]. Subsequently, the three-dimensional frame was installed at the construction site of the building and tested under dynamic vibration tests.

The building incorporates further innovative structural systems in the domain of hybrid or timber construction including a composite timber-concrete floor with beech-LVL, a hollow floor system with a prefabricated concrete top plate and a bottom plate in beech LVL and a bi-axial pure timber floor. Further details about these sub-structure systems can be found in [1]. The focus of this paper lies in the optimal sensor placement problem for the post-tensioned timber frame, although the described methodology could of course also be applied to the further systems involved, as well as the entire building.

2.2 Numerical Model in SAP2000

As an input to the OSP algorithms, the modal properties (fundamental frequencies and mode shapes) of the structure need to be quantified. The modal data can either be obtained from an analytical or numerical model, or from modal testing data. Here the algorithms are applied to modal data obtained from a numerical model of the structure realized in SAP2000. Three models were developed in SAP2000, namely, (i) a singlebay frame (2D), (ii) a three-bay frame (2D) (figure 1) and (iii) a three-dimensional grid of 8 frames. The last model corresponds to the actual building structure of the ETH HoNR (figure 2).

For all three models the same material properties were chosen. In the actual structure, the

Figure 3: Connection details

Table 1: Overview of model parameters

	1-bay frame	3-bay frame	3D frame
Modulus of elasticity E	$13kN/mm^2$	$13kN/mm^2$	$13kN/mm^2$
Weight	$5kN/m^3$	$5kN/m^3$	$5kN/m^3$
Column height	3m	3m	2.64m
Beam span	6.5m	6.5m	6.5m
Beam segments	4	4	4
Column segments	3	3	3
Number of Nodes	13	25	136
Analysis Type	2D (ux,uy,rotz)	2D (ux,uy,rotz)	3D (ux,uy,uz, rotx, roty, rotz)
DOFs (total)	39	75	816

columns are made of ash wood and the beams consist of a composite cross-section, with 4 lamellas in ash wood and the remaining lamellas in spruce. For simplicity reasons however, the entire structure was modelled as a single material with an elastic modulus of $13kN/mm^2$ and a weight of $5kN/m^3$ [9]. The cross-section of the columns for all models is 0.38m*0.38m and all beams are 0.28m deep and 0.72m high. For the single frame the span of the beam is 6.5m and the height of the columns 3m (analogue to the frame tested in the laboratory). The three-bay frame is modelled with the same geometry, by simply adding two more bays with a span of 6.5m, leading to a 19.5m long frame. The 3D frame spans 6.5m in two directions, leading to a 3 by 3 grid with outer dimensions of 19.5*19.5m. The column height for the 3D frame is 2.64m (analogue to the frame on the construction site).

Figure 3 illustrates the configuration of the joints of the frame. The bottom fixation is a doweled connection. For low-amplitude vibrations this connection acts as a rigid connection, and is therefore modelled as a fixed connection for all models. In order to include the effect of the post-tensioned joint into the model, a rotational spring is introduced on both ends of the beams, taking into account the moment-rotation stiffness of the connection (semi-rigid joint). In SAP2000 this connection is modelled as a partial release with a rotational stiffness. The stiffness values were chosen based on the laboratory tests on the single beam-column specimen [5] and from the pushover test on the 2D Frame [8]. For the 3D frame not only in-plane rotational releases are introduced, but also out-of plane rotational releases. The stiffness for the out-of plane release was analytically approximated from the in-plane stiffness based on geometrical relations. Table 1 provides an overview over the model parameters.

The OSP algorithms can be applied to any combination of possible sensor locations (degrees of freedom of the structure) and target modes, as long as the number of possible sensor positions is larger than the number of target modes. For demonstration purposes 3 target modes were defined for the 2D frames and 7 target modes for the 3D frame. Figure 4 illustrates the first three modes for all three systems, modes 4 to 7 of the 3D frame are not plotted herein; they were however considered for the optimization problem. The set of possible sensor locations is provided via the models from SAP2000. All beams and columns were discretized using several segments as indicated in Tab. 1, leading to a finite number of discrete nodes. Depending on the analysis type (2D or 3D), each node has either 3 or 6 degrees of freedom (DOFs), summing up to the total number of DOFs, i.e., possible candidate sensor locations per model. It is assumed that only 1-directional sensors will be positioned, recording accelerations or rotations only along one degree of freedom. In practical applications however, often tri-axial sensors are deployed. The interaction between translational and rotational degrees of freedom should then be taken into account, which is not possible with the herein described algorithms. A possible method for tackling this issue, namely the Tri-axial Effective Independence, is described in [10]. For the 2D frames a maximum number of 4 sensors was selected for the single span whilst 8 sensors were utilized for the 3-bay span, corresponding to an observation of 10% of the DOFs. For the 3D frame two different cases were considered, one monitoring of 1% of the DOFs (8 sensors) and one to 2% of the DOFs (16 sensors).

3 OPTIMAL SENSOR PLACEMENT

The OSP problem accepts a matrix $\mathbf{\Phi} \in \mathbb{R}^{m \times n}$ of target modes of interest, where m corresponds to the candidate sensor locations (FEM DOFs) and n to the number of modes, and aims at finding the best N positions to place sensors, where $m \ll N$ and $N \geq n$. All algorithms presented herein iteratively remove all candidate positions that do not significantly contribute to a specific metric.

3.1 The Effective Independence Method

The effective independence (EFI) method was developed by Kammer [11]. The algorithm calculates the Fisher Information Matrix as $\mathbf{A} = \mathbf{\Phi}^T\mathbf{\Phi}$ and then solves the eigenvalue problem for $\mathbf{A}$, $\mathbf{A\Psi} = \lambda\mathbf{\Psi}$. Accordingly, the EFI matrix is formulated as

$$\mathbf{EFI} = [\mathbf{\Phi\Psi}] \circ [\mathbf{\Phi\Psi}]\mathbf{\Lambda}^{-1} \tag{1}$$

where $\circ$ is the Hadamard product and $\mathbf{\Lambda}$ is the diagonal matrix of the eigenvalues of $\mathbf{A}$. Since $\mathbf{EFI}$ quantifies the contribution of every sensor to the associated eigenvalue, the column vector $\mathbf{E}_D$ (effective independence distribution vector) that results from summing up each row of $\mathbf{EFI}$ evaluates the candidate sensor location contributions; the candidate sensor position with the lowest contribution value is removed and the process is repeated until the rows of $\mathbf{E}_D$ reach the required number of sensors.

Figure 5 shows the results of the implementation of the EFI method on the three structural systems discussed. The arrows indicate the position and direction of the DOF to be monitored. N indicates the number of sensors placed and TM the number of target modes used as input for the OSP algorithm.

3.2 The EFI–DPR method

The driving point residue EFI (EFI–DPR) method is based on the original EFI method and proposes a weighted version of the original effective independence distribution vector, in which

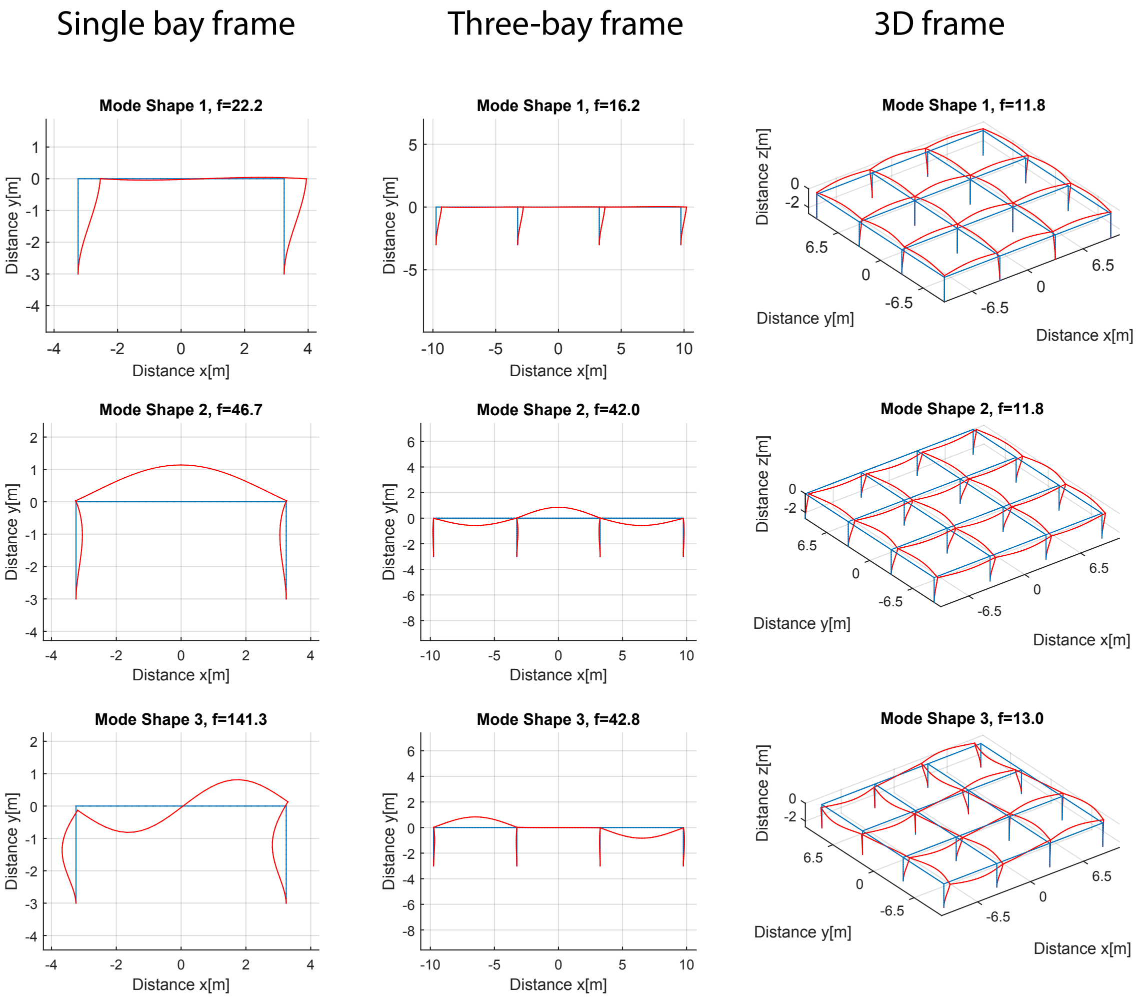

Figure 4: Mode shapes from the SAP models

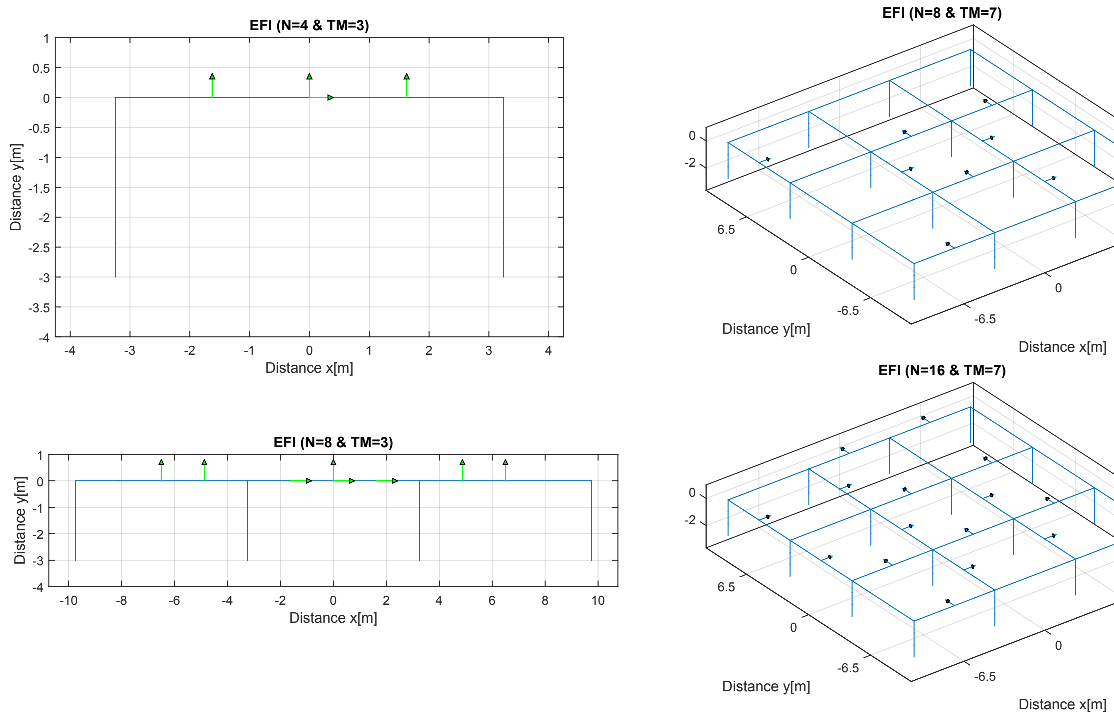

Figure 5: Optimal Sensor Positions from the EFI

the weights are calculated by the DPR coefficients as

$$DPR_i = \sum_{j=1}^{n} \frac{\Phi_{ij}^2}{\omega_j} \tag{2}$$

Figure 6 shows the results of the implementation of the EFI-DPR method on the three structural systems (N= number of monitored DOFs, TM = number of target modes).

3.3 The Maximum Kinetic Energy Method

The maximum kinetic energy (MKE) method implements a similar framework. However, instead of maximizing the Fisher Information matrix, the kinetic energy matrix is used [12, 3] instead:

$$\text{MKE} = \mathbf{\Phi}^T \circ \mathbf{M}\mathbf{\Phi} \tag{3}$$

where M is the mass matrix. Figure 7 shows the results of the implementation of the MKE method on the three structural systems (N= number of monitored DOFs, TM = number of target modes).

4 DISCUSSION

For the single span frame the first three modes were chosen as target modes. The first mode is a translational mode, which is captured by at least one horizontal sensor for all three methods. The EFI-DPR and the MKE method place two sensors in the horizontal direction. Indeed the OSP configurations are identical for the EFI-DPR and the MKE method. Two vertical sensors are placed at the quarter span in order to catch the beam deflection of the second and the third mode. The EFI method adds a third vertical sensor at mid-span in order to capture the second

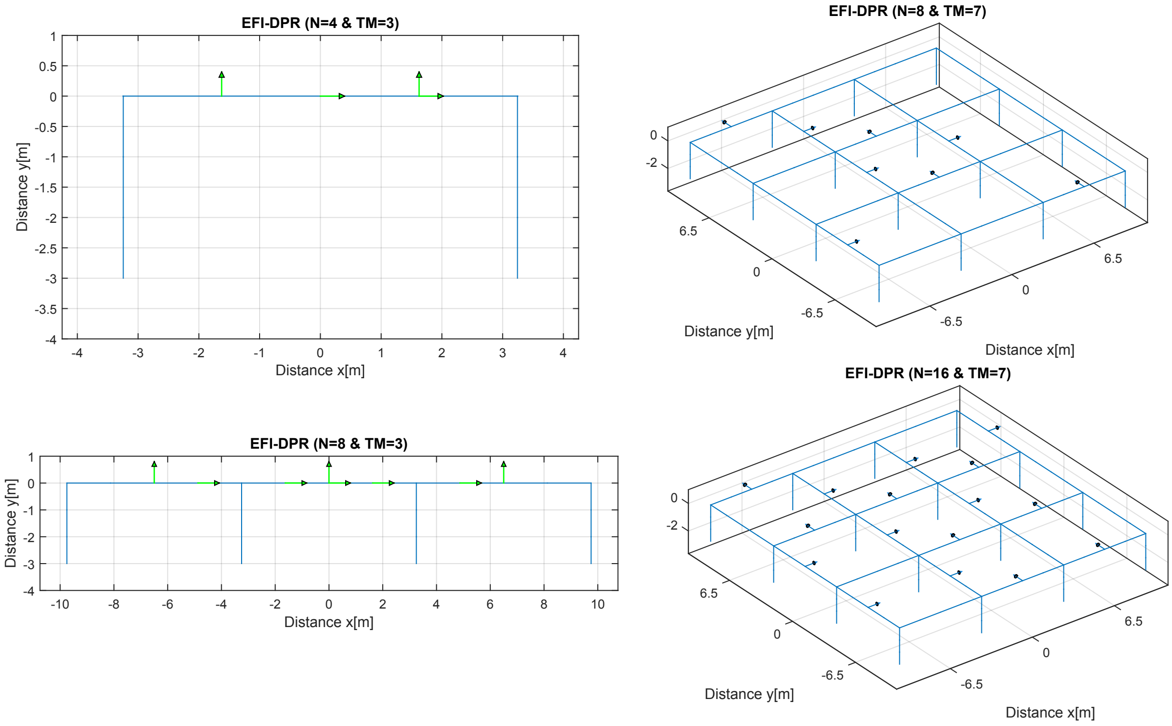

Figure 6: Optimal Sensor Positions from the EFI-DPR

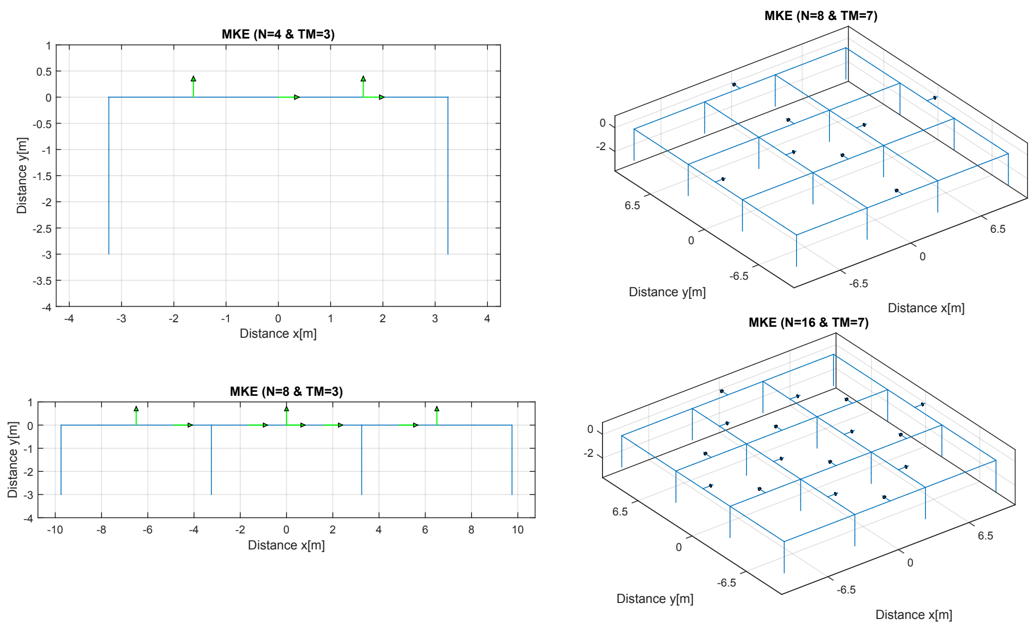

Figure 7: Optimal Sensor Positions from the MKE

mode and therefore allocates only one sensor in the horizontal direction. Since the columns exhibit only low deformations for the third mode shape, no sensors are placed on the columns.

For the three-bay span the first fundamental mode is also a horizontal translation of the beam. The second and third mode however exhibit mostly vertical deflections of the beam. The columns only deform in the first mode shape, at a lower amplitude then the local beam mode therefore no sensors are placed on the columns by any of the methods. Here however, also the column modes are of interest, particularly since the support conditions have a vital influence on the system behaviour. To this end, an amendment of the tested OSP methods should be considered in the future. Again the EFI-DPR and the MKE method give the same results. The EFI places three horizontal sensors and the other two methods place five horizontal ones in order to catch the first mode. The remaining sensors are then placed vertically at the beam mid-spans (EFI-DPR and MKE), or at the quarter spans (EFI). The EFI setup will therefore allow to gain more information on the deflection / modes of the beams then the EFI-DPR and the MKE setups.

Focusing on the 3D frame, all three methods yield different configurations for the sensors. The first two global modes of the 3D frame are a global translation and the third mode is a global rotation. In addition to these global deformations local deformations occur in the beams, mostly in the out-of plane direction. This is also captured by the OSP results. For all setups, sensors are always placed at the mid-span of the beams in the horizontal direction where the deflection is largest. No vertical sensors are placed, since the first seven mode shapes do not exhibit any vertical deflection. This is due to the lower stiffness of the column-beam joint in the out-of plane direction. This also explains why the placement of sensors is always perpendicular to the span direction. The change from 1% of DOFs to 2% of DOFs basically leads to a denser sensor coverage. Sensors are nearly evenly distributed in x and y direction, so that all translational and rotational modes can be captured.

While overall the OSP algorithms deliver reasonable placing results, some remaining issues deserve further investigation. In specific, one suggestion for better placement might be the separation of the global (translation and rotation of the entire frame grid) modes from the local beam modes. Since the sensors are placed on the mid-span of the beams they record a combination of the local beam mode and the global mode. In order to resolve this problem in the future, a sub-structuring of local and global modes might be of usage. Another issue of the above approach might be the sparse mesh used in the numerical model. Optimal positions might differ from quarter / third or mid-span. A possible solution to this problem would perhaps be to rerun separate elements using a denser mesh, although maintaining the number of sensors and the approximate locations per element that occurred through the sparser analysis. Indeed, if the OSP algorithms are directly employed on a dense mesh model, many neighbouring sensors will appear close to points of maximum deflection, instead of an even distribution over the entire structure. Further issues that should not be omitted are of course uncertainties in the modelling, so the sensor setup should be cross-checked with real measurement data, which would also allow to consider the influence of sensor noise or malfunctioning on the optimal sensor setup.

5 CONCLUSION

In the paper presented herein, three OSP algorithms are applied to numerical models of three different innovative timber structures. The obtained sensor setups can be used to determine the sensor setup for experimental tests on a 2D post-tensioned timber frame in the laboratory and for a 3D post-tensioned timber frame on the construction site of the ETH House of Natural Resources. The three OSP algorithms reveal a reasonable positioning of the sensors positions with results differing only slightly among different algorithms.

In the future, a similar OSP process will be further applied to the numerical model of the actual building structure of the ETH House of Natural Resources, leading to an optimal sensor setup, which minimizes intervention, for the long-term monitoring of the building. Furthermore, the idea is to rely on mode shapes that are not only from a baseline numerical model, but additionally from experimental data from the different construction stages of the building, hence leading to a multi-phase OSP problem.

REFERENCES

[1] Claude Leyder, Flavio Wanninger, Andrea Frangi, and Eleni Chatzi. Field testing on innovative timber structures. In *World Conference on Timber Engineering 2014*, 2014.

[2] Ting-Hua Yi and Hong-Nan Li. Methodology developments in sensor placement for health monitoring of civil infrastructures. *International Journal of Distributed Sensor Networks*, 2012:1–11, 2012.

[3] M. Meo and G. Zumpano. On the optimal sensor placement techniques for a bridge structure. *Engineering Structures*, 27(10):1488–1497, 2005.

[4] Robin S Glassburn and Suzanne Weaver Smith. Evaluation of sensor placement algorithms for on-orbit identification of space platforms. 1994.

[5] F Wanninger and A Frangi. Experimental and analytical analysis of a post-tensioned timber connection under gravity loads. *Engineering Structures*, 70:117–129, 2014.

[6] Andy Buchanan, Bruce Deam, Massimo Fragiacomo, Stefano Pampanin, and Alessandro Palermo. Multi-storey prestressed timber buildings in new zealand. *Structural Engineering International*, 18(2):166–173, 2008.

[7] A Buchanan, A Palermo, D Carradine, and S Pampanin. Post-tensioned timber frame buildings. *Structural Engineer*, 89(17):24–30, 2011.

[8] Fabio Steiner. *Evaluation of full-scale tests on a post-tensioned timber frame*. Master Thesis. ETH Zürich., 2014.

[9] EN DIN. 338: 2010-02: Structural timber-strengt classes; german version en 338: 2009, din deutsches institut fr normung e. *V., Berlin, Germany*, 2010.

[10] Daniel C Kammer and Michael L Tinker. Optimal placement of triaxial accelerometers for modal vibration tests. *Mechanical systems and signal processing*, 18(1):29–41, 2004.

[11] Daniel C. Kammer. Sensor placement for on-orbit modal identification and correlation of large space structures. *Journal of Guidance, Control, and Dynamics*, 14(2):251–259, 1991.

[12] G Heo, ML Wang, and D Satpathi. Optimal transducer placement for health monitoring of long span bridge. *Soil dynamics and earthquake engineering*, 16(7):495–502, 1997.